



Recombinant Spider Silk–Silica Hybrid Scaffolds with Drug-Releasing Properties for Tissue Engineering Applications

Sushma Kumari, Hendrik Bargel, and Thomas Scheibel*

Fabricating biomaterials with antimicrobial activity to prevent the growth of detrimental microorganisms is of great scientific and practical interest. Here, composite materials comprising recombinant spider silk proteins and mesoporous silica nanoparticles (MSN) loaded with selected antibiotics and antimycotics are fabricated into films and hydrogels. The derived composite materials exhibit excellent antimicrobial properties with sustained release of antibiotics over the course of 15 days. Furthermore, antibiotics/antimycotics inclusion does not impair the cytocompatibility of the composite materials, all of which promote fibroblast cell adhesion and proliferation. Finally, processing of spider silk–MSN composite hydrogels using 3D printing is shown to enable the fabrication of patient-specific antimicrobial implants to prevent infection in the near future.

Antimicrobial modification of surfaces to inhibit bacterial or fungal colonization is a highly desired objective in medicine. Microbial attachment and subsequent microbial colonization as well as biofilm formation on surfaces, for example, of medical equipment, leads to the transmission of community-acquired or hospital-acquired (nosocomial) infections deteriorating public health and impeding healthcare, cosmetics and technical applications.^[1,2] Bacterial infections based on biomedical implants and devices are one of the growing problems leading to the failure of implants and promoting the chances of revision surgery.^[3,4]

Antibiotics are widely used as a treatment to cure microbial infections, and their incorporation into films for coating

of other materials as well as scaffolds, for example, for tissue regeneration are among the most promising strategies to prevent microbial colonization.^[5] Unfortunately, the emergence of drug-resistant strains as well as the insufficient activity or concentration of antibiotics at the site of infection lead to their failure in clinical treatment.^[6,7] Different strategies have been developed to achieve a long-term antibiotic therapy, such as chemical modification of antibiotics, development of new antimicrobial agents, and new formulation methods for antibiotic delivery.^[8–11] Nanomaterials can also be used in drug formulations, enabling the development

of targeted delivery systems to the site of infection, minimizing nonspecific interactions, and controlling delivery of antibiotics mitigating the development of microbial resistance and other side effects experienced with traditional therapies.^[10,12–15] Nanocarriers also allowed combination therapy with multi-antibiotics delivery and flexibility of the dosage amount.^[16,17]

In the last decade, mesoporous silica nanoparticles (MSN) have been explored as nanovehicles for delivery of antibiotics and other drugs due to several advantageous properties, such as a high surface area, large pore volume, tunable particle and pore size, and easy surface functionalization.^[18–20] Using MSN, antibiotic delivery systems have been prepared through various techniques, for example, functionalized or adsorbed antimicrobials on the surface, encapsulating the active molecule within the nanoparticles, chemically conjugating antimicrobials to particles surface, and depositing drugs using layer-by-layer (LbL) assembly.^[14,19]

Here, we designed enhanced antimicrobial composite materials for sustainable drug release to combat bacterial and fungal infections by combining the engineered spider silk protein eADF4(C16) and antimicrobials loaded MSN. eADF4(C16) is a recombinant spider silk protein based on the consensus sequence of the core domain of *Araneus diadematus* fibroin 4 (ADF4) of the dragline silk of the European garden spider *A. diadematus*.^[21] eADF4(C16)-based materials present interesting properties such as biocompatibility, absence of toxicity, low/non-immune reactivity, and controlled biodegradability.^[22–24] Furthermore, eADF4(C16) can be fabricated into different morphologies like films,^[25,26] non-woven mats,^[27] hydrogels,^[28] foams,^[29] and bioinks,^[30] and can be used as coating materials for implants^[31,32] and other biomedical products.^[26]

The utilization of spider silk–MSN composites as antimicrobial materials were demonstrated by encapsulating a variety of aminoglycoside antibiotics and antimycotics as shown in

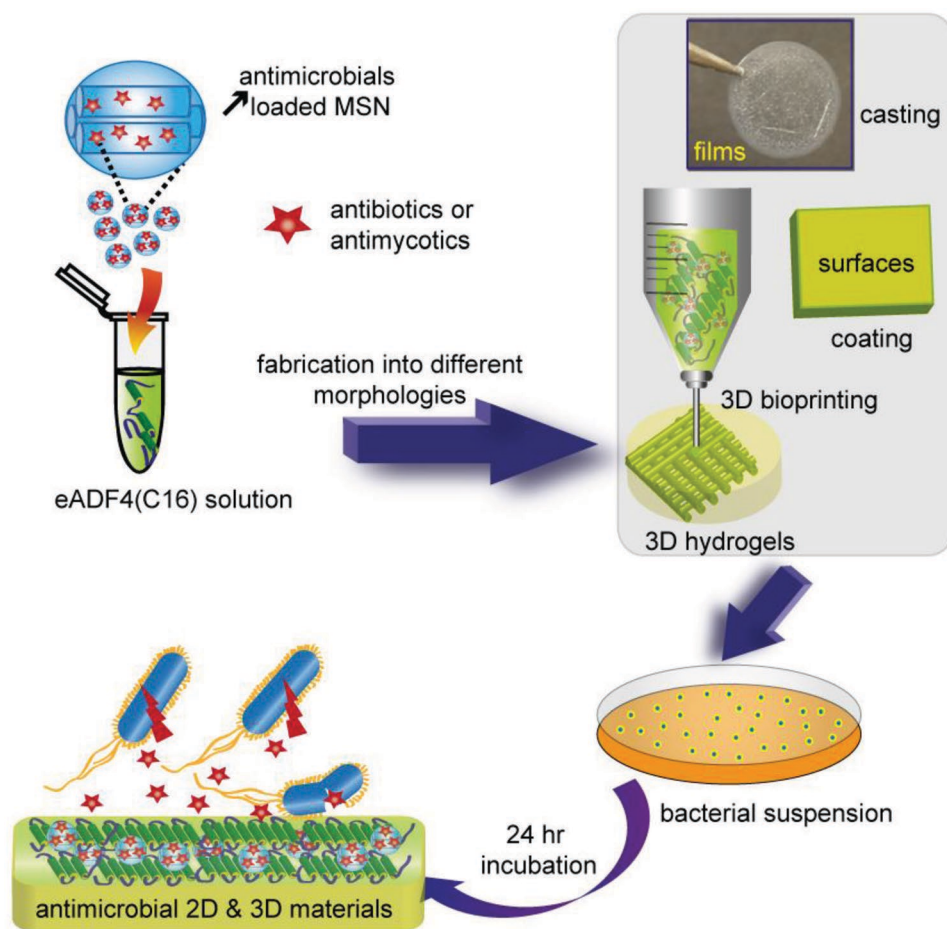
Dr. S. Kumari, Dr. H. Bargel, Prof. T. Scheibel
Department of Biomaterials
Faculty of Engineering Science
Prof.-Rüdiger-Bormann-Str. 1
University of Bayreuth
95447 Bayreuth, Germany
E-mail: thomas.scheibel@bm.uni-bayreuth.de

Prof. T. Scheibel
Bayreuth Center for Material Science and Engineering (BayMAT)
Bavarian Polymer Institute (BPI)
Bayreuth Center for Colloids and Interfaces (BZKG)
Bayreuth Center for Molecular Biosciences (BZMB)
University of Bayreuth
95447 Bayreuth, Germany

The ORCID identification number(s) for the author(s) of this article can be found under <https://doi.org/10.1002/marc.201900426>.

© 2019 The Authors. Published by WILEY-VCH Verlag GmbH & Co. KGaA, Weinheim. This is an open access article under the terms of the Creative Commons Attribution-NonCommercial-NoDerivs License, which permits use and distribution in any medium, provided the original work is properly cited, the use is non-commercial and no modifications or adaptations are made.

DOI: 10.1002/marc.201900426



Scheme 1. Schematic representation of drug-loaded recombinant spider silk-mesoporous silica nanoparticles (MSN) composite films and hydrogels with anti-microbial properties.

Scheme 1. The spider silk–MSN (SM) composite films were further used to coat polymeric, metallic, as well as ceramic materials to show their efficacy in killing bacteria and fungi. Selected antibiotics, namely gentamicin (G), kanamycin (K), and neomycin (N), and the antimycotic amphotericin B (A), possess biologic activities rendering them successful disinfectants, antiseptic and anti-inflammatory agents. Antibiotic activity of the SM composites was evaluated based on the growth inhibition of *Escherichia coli* (*E. coli*) and *Pichia pastoris* (*P. pastoris*). SM composites showed excellent performance in terms of antimicrobial properties including their minimum inhibitory concentrations (MICs) and surface antimicrobial activities against *E. coli* and *P. pastoris*.

Spherical MSN with a particle size of 72 ± 5 nm were synthesized through a sol–gel process and characterized using scanning electron microscopy (SEM) and transmission electron microscopy (TEM), Figure S1, Supporting Information.^[33,34] MSN were loaded with aminoglycoside antibiotics (gentamicin, neomycin, and kanamycin) and antimycotics (Amphotericin B) dissolved in Tris buffer (10 mM, pH 7.5) via diffusion upon incubation for 24 h at 37 °C. Loading of antibiotics onto silica particles is highly favorable as aminoglycoside antibiotics/antimycotics contain a hydroxyl as well as secondary amine

groups, initiating supramolecular interactions between the drug and silica matrices (electrostatic interactions, hydrogen bonding, π – π stacking, etc.). The loading amount was calculated to be 400 μ g gentamicin (G), 350 μ g neomycin (N), 390 μ g kanamycin (K), and 6.2 μ g Amphotericin B (A) per mg MSN, respectively, Figure S2, Supporting Information.

Antibiotics and antimycotics loaded MSN were mixed with 4% w/v recombinant spider silk solution, and composite films were made by drop casting followed by post-treatment with ethanol. The presence of silica nanoparticles in the spider silk matrix was confirmed SEM, atomic force microscopy (AFM), and Fourier transform infrared (FT-IR) spectroscopy, as shown in Figure 1a,b; Figure S3, Supporting Information. Minimum inhibitory concentrations (MICs) of the antibiotics/antimycotics loaded SM composite films were evaluated using liquid cultures of *E. coli* and *P. pastoris*, respectively. After 24 h, the optical density at 600 nm (OD_{600}) of the bacterial/yeast cell suspension in contact with the film showed a significant decline in the bacterial and yeast cell growth with increasing concentration of antibiotics/antimycotics loaded MSN particles in the composite films, Figure 1c,d. Therefore, SM composite films with sufficient drug concentrations are able to significantly suppress microbial growth in the surrounding solution.

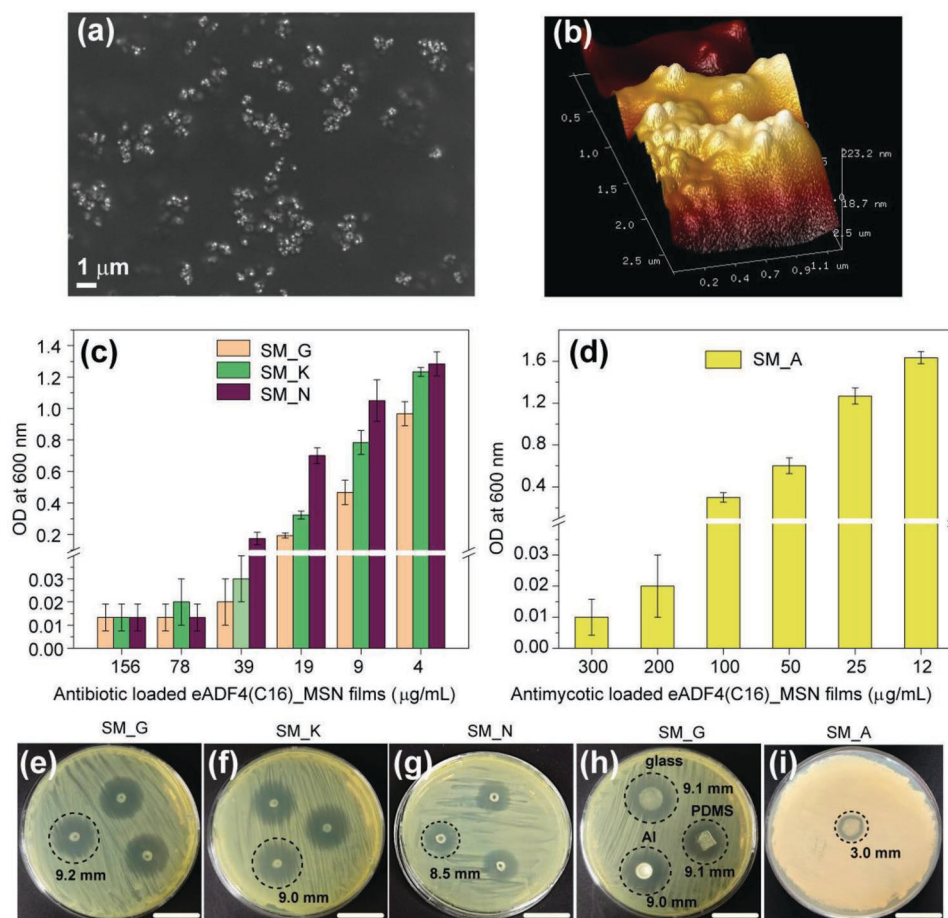


Figure 1. a) SEM images of eADF4(C16)_MSN (SM) films. b) Tapping mode atomic force microscopy images showing the topography of SM films on Si wafer. The average surface roughness R_a of 180 nm was calculated at an area of $9 \mu\text{m}^2$. c,d) Antibacterial/antifungal activity of antibiotics (gentamicin (G), kanamycin (K), neomycin (N)), and antimycotic (Amphotericin B (A)) loaded SM composite films in a concentration dependent manner. Turbidity of *E. coli* suspensions in Luria–Bertani (LB) medium at 37°C and *P. pastoris* in yeast extract–peptone–dextrose (YPD) medium at 30°C were measured at 600 nm (OD_{600}) after 24 h incubation. The results are expressed as mean \pm SD, and experiments were done in triplicate with a minimal sample number of three. e–h) Inhibition zone test of antimicrobial loaded SM films and film coated surfaces using *E. coli* on agar plates; e) SM_G free standing films; f) SM_K free standing films; g) SM_N free standing films, h) SM_G coated material surfaces (glass, Al and PDMS), and i) SM_A free-standing films using *P. pastoris* on an agar plate. Black dotted circles represent the inhibition zone area. Scale bars (e–i): 2 cm.

The antimicrobial properties of films and coatings were prepared using a 4% w/v eADF4(C16) solution mixed with 0.5% w/v MSN loaded with antibiotics or antimycotic and were tested using a zone of inhibition test on agar plates. All free-standing silk–silica composite films of SM_G, SM_K, and SM_N were placed on *E. coli*-inoculated agar plates and SM_A films on *P. pastoris*-inoculated agar plates and incubated for 12 h at 37°C . Antimicrobial activity of the films could be seen as prominent zone of inhibition rings around films, Figure 1e–g,i. Significant inhibition zones with diameters of 8–9 mm were observed for SM_G, SM_K, and SM_N, and 3 mm for SM_A. The smaller inhibition zone observed for SM_A is due to the very low solubility of Amphotericin B in water. Importantly, recombinant spider silk films without MSN did not have any detectable inhibition zone (Figure S4, Supporting Information) indicating that recombinant spider silk materials cannot actively reduce already existing infections. Next, we tested the ability of the SM composite films

to serve as antibacterial coatings on other materials such as glass, aluminum (Al), and polydimethylsiloxane (PDMS), all processed by dip coating. SEM microscopy analysis depicted smooth and crack-free coatings on the materials surfaces (Figure S5, Supporting Information). Also, no bacterial growth was observed on top of the coatings or adjacent to the coatings (zone of inhibition) after 24 h incubation, Figure 1h. Coated surfaces resisted biofilm formation. Therefore, SM composite coatings can be used in the future to improve the efficacy of medical devices and implants.

To fabricate SM composite hydrogels, 1% w/v MSN loaded with antibiotics or antimycotic were added to aqueous solutions of 4% w/v eADF4(C16) under static conditions, followed by gelation of the silk at 37°C . The morphology of the MSN-loaded freeze-dried eADF4(C16) hydrogel was investigated by SEM (Figure S6, Supporting Information). The time-dependent antimicrobial efficacy of SM composite hydrogels was tested using zone of inhibition tests against *E. coli* and *P. pastoris*

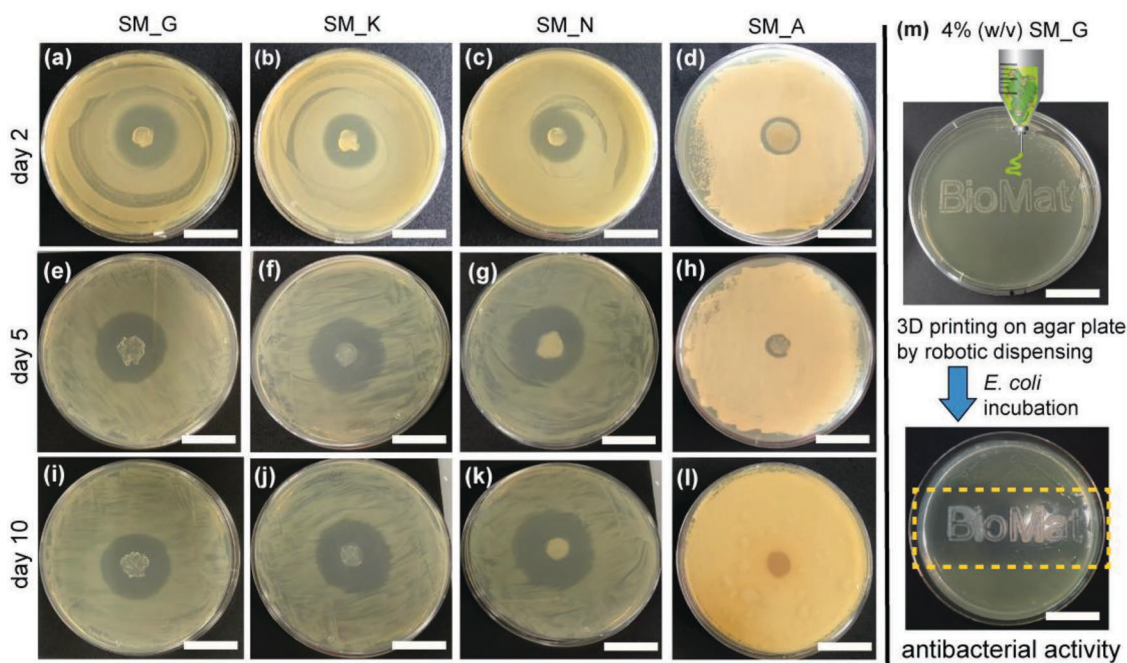


Figure 2. Inhibition zone test of antimicrobial loaded SM hydrogels using *E. coli* and *P. pastoris* on agar plates to show the sustainability of antimicrobial release. a–d) Hydrogels after 2 days of incubation in PBS: a) SM_G, b) SM_K, c) SM_N, and d) SM_A. Similarly, inhibition zone tests were performed for antimicrobial-loaded SM hydrogels after incubation in PBS on e–h) day 5 and i–l) day 10. 3D printing of (m) 4% w/v gentamicin (G) loaded SM_G hydrogel on an agar plate. After printing, *E. coli* bacteria culture ($OD_{600} = 1.0$) was spread on the plates and incubated overnight at 37 °C. The dotted rectangular area shows the inhibition zone for the growth of *E. coli* bacteria on the agar plate. Scale bars: 2 cm.

on agar plates. Antimicrobials loaded SM hydrogels were first incubated in PBS (25 mM K-Phos, 100 mM NaCl, pH 7.5) for 10 days and then removed to test their remaining antibacterial or antifungal properties on day 2, day 5, and day 10 on agar plates inoculated with bacteria or yeast, **Figure 2a–l**. Inhibition zones around SM composite hydrogels showed that the activity of antibiotics and antimycotics was retained within the hydrogels even after 10 days of incubation in PBS and demonstrated its usability for long-term antimicrobial activity against microbial infection. Also, the *in vitro* release behavior of antibiotics from MSN embedded in 4% w/v eADF4(C16) hydrogels were analyzed in PBS. The release profile showed a slow and continuous release of antibiotics over 14 days, with a release of gentamicin, neomycin, and kanamycin of 34%, 29%, and 38%, (Figure S7, Supporting Information). The slow release of antibiotics suggested that silk–silica composite hydrogels can be used as a drug delivery system to achieve sustained release of drugs, and administering drugs systemically to avoid side effects due to high local concentrations.

To illustrate the versatility of this approach, recombinant SM composite hydrogels were 3D printed. The concept is demonstrated in **Figure 2m** with 3D printed constructs using robotic dispensing of gentamicin loaded silk–silica (SM_G) composite hydrogels on an agar plate. Introduction of *E. coli* to the 3D printed constructs after printing resulted in a well-defined inhibition zone demonstrating that the antibacterial activity was retained after printing. 3D printing of SM composites holds the potential toward fabrication of anti-infective scaffolds with integrated drugs for biomedical applications.

A high dose of antibiotics might significantly interfere with cell replication and even cause cell death. Therefore, we studied the cytotoxicity of antimicrobial loaded spider silk–MSN films using fibroblasts, which are one of the first anchorage-dependent cells to interact with an implant surface during the wound healing process. Recombinant spider silk protein eADF4(C16) lacks cell binding motifs, however, materials made of the genetically modified variant eADF4(C16)-RGD have shown high potential for tissue engineering applications.^[29,30,35] Films and hydrogels made of eADF4(C16)-RGD have previously been thoroughly characterized, and studies showed no significant differences in their physicochemical properties as well as secondary structure in comparison to eADF4(C16).^[35–37] The viability of BALB/3T3 cells was evaluated on films of eADF4(C16)-RGD with encapsulated antimicrobial loaded nanoparticles analysing their mitochondrial activity. No cytotoxicity could be detected, **Figure 3a**. In addition, proliferation was good on the respective films (**Figure 3b,d–f**) and within the hydrogels (**Figure 3c,g–i**).

Novel drug-eluting composite materials were prepared by combining recombinant spider silk eADF4(C16) and antimicrobial agents loaded MSN to prevent biofilm formation. Spider silk–MSN (SM) composites films and hydrogels exhibited long-lasting antimicrobial properties against *E. coli* and *P. pastoris*. In addition, the composites could be processed into coatings on glass, metals, and PDMS, and exhibited there also long-lasting antibacterial properties. Release profiles of antibiotics-loaded composite hydrogels demonstrated the preserved antibacterial potency over 2 weeks via sustained release

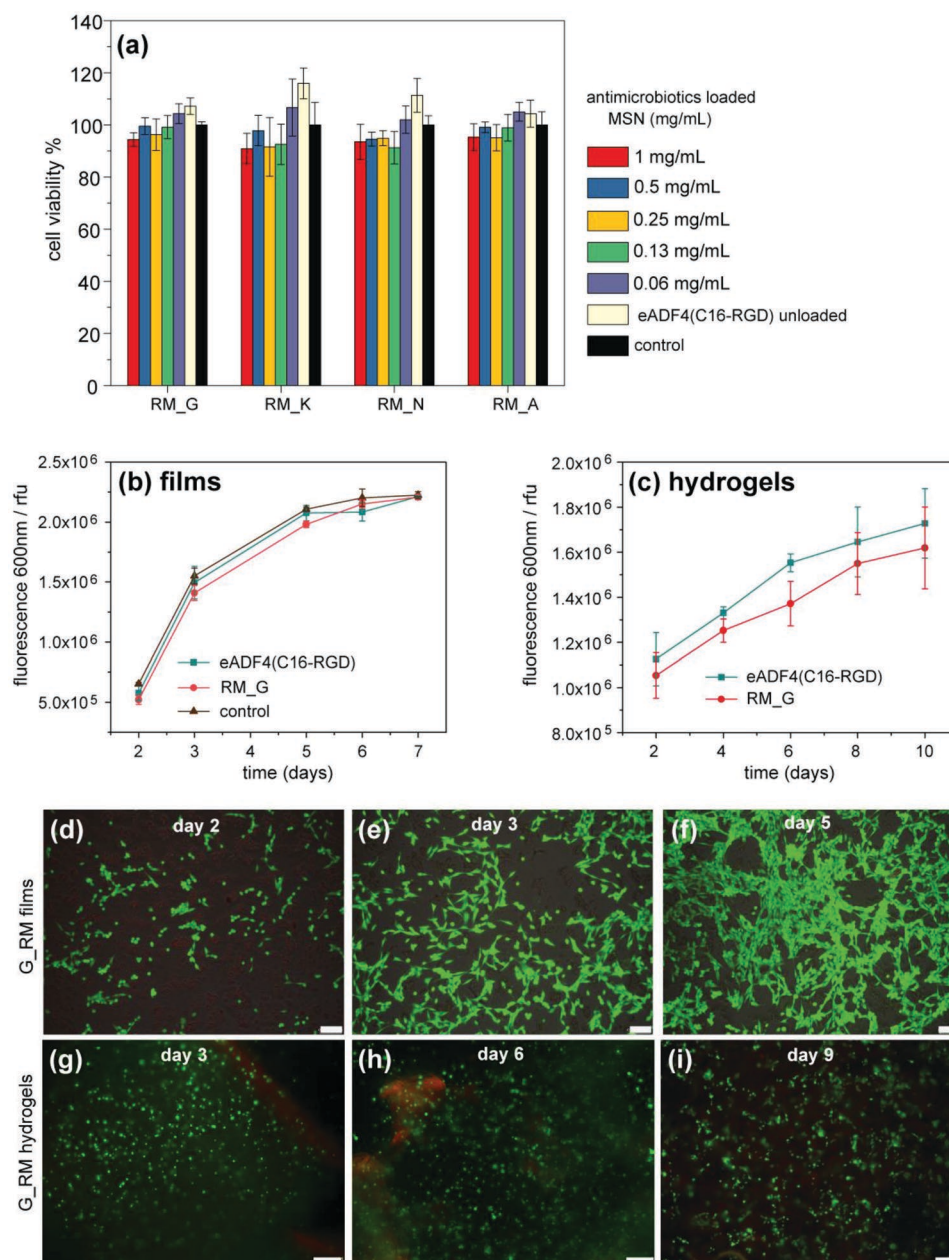


Figure 3. a) Cell viability of mouse BALB/3T3 fibroblasts cultured on films of antimicrobial loaded eADF4(C16)-RGD_MSN (RM) films (antimicrobials concentration as indicated) was quantified using the Cell-titer blue assay after 48 h of incubation at 37 °C. Cell-viability was normalized with cells cultured on treated well plates (positive control). b,c) Proliferation of BALB/3T3 fibroblasts on films and hydrogels over 5 and 10 days, respectively, was quantified using the cell-titer blue assay. Live-dead cell microscopy of mouse BALB/3T3 fibroblasts cultivated on d–f) composite silk–silica films and g–i) composite silk–silica hydrogels. Scale bars: d–f) 100 μ m and g–i) 250 μ m. The cells were stained with calcein A/M (live cells: green) and ethidium homodimer I (dead cells: red). Ethidium homodimer I also stained the hydrogels yielding an unspecific red background fluorescence (g–i).

of antibiotics. Furthermore, 3D printed SM composite hydrogels showed zones of inhibition upon direct contact with *E. coli*. Combining such SM composites with 3D printing enables fabrication of patient-specific antimicrobial implants to prevent infection. Additionally, the potential of drug-eluting SM composite scaffolds was revealed in the context of biomedical and wound healing processes. In summary, this study demonstrates putative applications for SM composites that

may be used in various biomedical applications and as coatings for surgical tools.

Supporting Information

Supporting Information is available from the Wiley Online Library or from the author.

Acknowledgements

The authors thank Tamara Aigner for TEM imaging, Sarah Lentz for AFM measurements, and Dr. Elise Liensdorf for help in 3D printing. This work was supported by the German Research Foundation (DFG) grant SFB 840 TP A8 and European Union Grand ETZ-EFRE 2014–2020, Freistaat Bayern–Tschechien, Project Nr. 123.

Conflict of Interest

Thomas Scheibel is founder and shareholder of AMSilk GmbH, Germany.

Keywords

antimicrobials, films, hydrogels, mesoporous silica nanoparticles, recombinant spider silk protein

Received: August 16, 2019

Revised: September 24, 2019

Published online: November 7, 2019

- [1] M. E. Davey, G. A. O'toole, *Microbiol. Mol. Biol. Rev.* **2000**, *64*, 847.
- [2] L. Hall-Stoodley, J. W. Costerton, P. Stoodley, *Nat. Rev. Microbiol.* **2004**, *2*, 95.
- [3] R. A. Weinstein, R. O. Darouiche, *Clin. Infect. Dis.* **2001**, *33*, 1386.
- [4] S. Veerachamy, T. Yarlagadda, G. Manivasagam, P. K. Yarlagadda, *Proc. Inst. Mech. Eng., Part H* **2014**, *228*, 1083.
- [5] M. Zilberman, J. J. Elsner, *J. Controlled Release* **2008**, *130*, 202.
- [6] C. Baker-Austin, M. S. Wright, R. Stepanauskas, J. V. McArthur, *Trends Microbiol.* **2006**, *14*, 176.
- [7] A. P. Magiorakos, A. Srinivasan, R. B. Carey, Y. Carmeli, M. E. Falagas, C. G. Giske, S. Harbarth, J. F. Hindler, G. Kahlmeter, B. Olsson-Liljequist, D. L. Paterson, L. B. Rice, J. Stelling, M. J. Struelens, A. Vatopoulos, J. T. Weber, D. L. Monnet, *Clin. Microbiol. Infect.* **2012**, *18*, 268.
- [8] P. Gao, X. Nie, M. Zou, Y. Shi, G. Cheng, *J. Antibiot.* **2011**, *64*, 625.
- [9] A. J. Huh, Y. J. Kwon, *J. Controlled Release* **2011**, *156*, 128.
- [10] N. Abed, P. Couvreur, *Int. J. Antimicrob. Agents* **2014**, *43*, 485.
- [11] E. M. Hetrick, M. H. Schoenfish, *Chem. Soc. Rev.* **2006**, *35*, 780.
- [12] R. Y. Pelgrift, A. J. Friedman, *Adv. Drug Delivery Rev.* **2013**, *65*, 1803.
- [13] F. Nederberg, Y. Zhang, J. P. K. Tan, K. Xu, H. Wang, C. Yang, S. Gao, X. D. Guo, K. Fukushima, L. Li, J. L. Hedrick, Y.-Y. Yang, *Nat. Chem.* **2011**, *3*, 409.
- [14] Y. Liu, L. Shi, L. Su, H. C. van der Mei, P. C. Jutte, Y. Ren, H. J. Busscher, *Chem. Soc. Rev.* **2019**, *48*, 428.
- [15] N. Beyth, Y. Hourri-Haddad, A. Domb, W. Khan, R. Hazan, *Evidence-Based Complementary Altern. Med.* **2015**, *2015*, 246012.
- [16] L. Ejim, M. A. Farha, S. B. Falconer, J. Wildenhain, B. K. Coombes, M. Tyers, E. D. Brown, G. D. Wright, *Nat. Chem. Biol.* **2011**, *7*, 348.
- [17] A. Gupta, S. Mumtaz, C.-H. Li, I. Hussain, V. M. Rotello, *Chem. Soc. Rev.* **2019**, *48*, 415.
- [18] J. G. Croissant, Y. Fatieiev, A. Almalik, N. M. Khashab, *Adv. Healthcare Mater.* **2018**, *7*, 1700831.
- [19] A. Bernardos, E. Piacenza, F. Sancenón, M. Hamidi, A. Maleki, R. J. Turner, R. Martínez-Máñez, *Small* **2019**, *15*, 1900669.
- [20] M. Vallet-Regí, M. Colilla, B. González, *Chem. Soc. Rev.* **2011**, *40*, 596.
- [21] D. Huemmerich, C. W. Helsen, S. Quedzuweit, J. Oschmann, R. Rudolph, T. Scheibel, *Biochemistry* **2004**, *43*, 13604.
- [22] K. Spiess, A. Lammel, T. Scheibel, *Macromol. Biosci.* **2010**, *10*, 998.
- [23] A. Leal-Egaña, T. Scheibel, *Biotechnol. Appl. Biochem.* **2010**, *55*, 155.
- [24] S. Müller-Herrmann, T. Scheibel, *ACS Biomater. Sci. Eng.* **2015**, *1*, 247.
- [25] D. Huemmerich, U. Slotta, T. Scheibel, *Appl. Phys. A* **2006**, *82*, 219.
- [26] C. B. Borkner, S. Wohlrab, E. Möller, G. Lang, T. Scheibel, *ACS Biomater. Sci. Eng.* **2017**, *3*, 767.
- [27] A. Leal-Egaña, G. Lang, C. Mauerer, J. Wickinghoff, M. Weber, S. Geimer, T. Scheibel, *Adv. Eng. Mater.* **2012**, *14*, B67.
- [28] K. Schacht, T. Scheibel, *Biomacromolecules* **2011**, *12*, 2488.
- [29] K. Schacht, J. Vogt, T. Scheibel, *ACS Biomater. Sci. Eng.* **2016**, *2*, 517.
- [30] K. Schacht, T. Jüngst, M. Schweinlin, A. Ewald, J. Groll, T. Scheibel, *Angew. Chem., Int. Ed.* **2015**, *54*, 2816.
- [31] P. Zeplin, N. Maksimovikj, M. Jordan, J. Nickel, G. Lang, A. Leimer, L. Römer, T. Scheibel, *Adv. Funct. Mater.* **2014**, *24*, 2658.
- [32] P. Zeplin, A. Berninger, N. Maksimovikj, P. van Gelder, T. Scheibel, H. Walles, *Handchir. Mikrochir. Plast. Chir.* **2014**, *46*, 336.
- [33] R. Mortera, J. Vivero-Escoto, I. I. Slowing, E. Garrone, B. Onida, V. S. Y. Lin, *Chem. Commun.* **2009**, *22*, 3219.
- [34] S. Kumari, B. B. Dhar, C. Panda, A. Meena, S. S. Gupta, *ACS Appl. Mater. Interfaces* **2014**, *6*, 13866.
- [35] S. Wohlrab, S. Müller, A. Schmidt, S. Neubauer, H. Kessler, A. Leal-Egaña, T. Scheibel, *Biomaterials* **2012**, *33*, 6650.
- [36] E. DeSimone, K. Schacht, T. Scheibel, *Mater. Lett.* **2016**, *183*, 101.
- [37] E. DeSimone, K. Schacht, A. Pellert, T. Scheibel, *Biofabrication* **2017**, *9*, 044104.